Malaysian Journal of Fundamental & Applied Sciences

available online at http://mjfas.ibnusina.utm.my

Fabrication and characterization of ferrites (Mg and Mn) based on FTIR, XRD, SEM and TEM

Tang Ing Hua* and Rita Sundari

Department of Chemistry, Faculty of Science, UTM, 81310 UTM Skudai, Johor, Malaysia

Received 7 January 2012, Revised 16 March 2012, Accepted 5 April 2012, Available online 28 April 2012

ABSTRACT

This study has encountered with the fabrication of ferrites (Mg and Mn) using citric acid as anionic surfactant in sol-gel method followed by calcinations at varied temperatures (300, 600, 800°C) for 2h, respectively. The fabricated ferrites have been characterized by FTIR (Fourier Transform Infrared Spectroscopy), XRD (X-Ray Diffraction), SEM (Scanning Electron Microscope) and TEM (Transmission Electron Microscope). The FTIR spectrum for $MnFeO_3$ shows that some functional groups already removed under 300°C calcination due to several oxidation numbers possessed by Mn leading to more flexibility. The XRD diffractograms for both $MgFe_2O_4$ and $MnFeO_3$ show that the transition phase from amorphous to crystalline structure occurred in the temperature range of 300-600°C. The SEM mappings based on the Fe distribution for both $MgFe_2O_4$ and $MnFeO_3$ show that more Fe distributed over the ferrites surface at 600 and 800°C, while the SEM mappings for both ferrites (Mg and Mn) show less Fe distribution at 300°C calcination, thus, it indicates more repulsion force bearing by higher amounts of Fe atoms at higher thermal agitation due to volume expansion. The TEM spectra proved that both ferrites existed as crystals after calcined at 600°C. The fabricated ferrites have remarkable electrical properties useful for the manufacture of semiconducting materials.

| sol gel method | calcinations | ferrites characterization. |

http://dx.doi.org/10.11113/mjfas.v8n3.140

1. INTRODUCTION

It has been known that spinel ferrites, with the general formula, MFe_2O_4 (M= Co, Zn, Mg, etc.), possess important electrical and magnetic properties, where they form close packed face-centered cubic (fcc) crystals while the M^{2+} and Fe^{3+} ions can form either tetrahedral or octahedral structures placed inside the fcc unit cell (Figure 1). On the other hand, perovskite ferrites, with the general formula, $MFeO_3$ (M= larger cation than Fe^{3+}, which is capable to form 12-fold coordination with oxygen), is more suitable for octahedral coordination exist in cubic crystals [1]. Generally, perovskite structures are more flexible since they can exist in one or more structural phase transitions particularly at lower temperature [2]. Both Mg- and Mn-ferrites have been found in broad applications including heterogeneous catalysts, sensors, and semiconductors [3]. Moreover, nanostructure ferrite materials have attracted great attentions due to their remarkable properties encountered with their impressive magnetic and electrical behaviors [4].

The electrical and magnetic properties of ferrites depend on their size, shape, crystalline structure and cationic distributions, which can be controlled during fabrication process.

Corresponding author at:
E-mail addresses: et_87@live.cn (Tang Ing Hua)

Metal nitrates have been found to be used as the starting material in the previous study using thermal method [5], polymerized complex method [6], simple salt method [7], electrospinning method [4], sol-gel method [8,9] and high energy ball milling method applying high sintering temperature [10,11]. Other miscellaneous methods related to ferrites fabrication, i.e. the soft mechanochemical method, which involved low sintering temperature [12], reverse micelle method with metal sulphate as starting materials [13], solid state reaction method [14], co-precipitation method with manganese ores as starting material followed by high calcination temperature [15] were reported in previous investigations.

Previous studies show that the crystalline ferrite will be formed at temperature above 500°C, with average crystalline size below 100nm [7,4, 5,16,]. The Increase in calcination temperature lead to increase in the size of crystal [4,5]. High calcination temperature lead to the existence of mixture of single crystal and multicrystal structure [10]. By applying the Vibrating Sample Magnetometer (VSM) increase in milling time caused to the increase in magnetisation [12]. The magnetic moment depends on the particle grain size and cation distribution. The decrease in the number of structural matters surround particles had led to the magnetization reduction in ferrite- nanoparticles [16]. While [4] obtained magnetisation value getting increased by increasing the calcinations temperature (500 – 800°C).

The important features of Mg- and Mn-ferrites have been viewed in this study where both ferrites are prepared by sol-gel method using citric acid anionic surfactant to aid the mixing process. The fabrication is accomplished by calcinations at varied temperatures (300, 600 and 800°C). The effects of calcinations are characterized by FTIR, XRD, SEM and TEM, and will be the subject to be highlighted in this study.

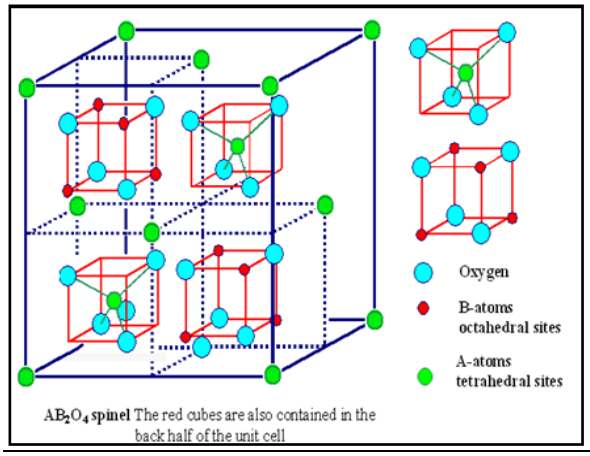

Fig. 1 Framework for spinel lattice cell with tetrahedral and octahedral inside the lattice.

2. EXPERIMENTAL

2.1 Materials, method and instruments

The chemicals, $Fe(NO_3)\cdot 9H_2O$ (OReC,Grade AR), $Mg(NO_3)_2\cdot 6H_2O$ pure (HmbG), MnO_2 (MERCK Schuchard OHG, Germany), $C_6H_8O_7\cdot H_2O$ (OReC, Grade AR) were selected as precursors in this investigation. Fourier Transform Infrared spectroscopy, FT-IR (Perkin Elmer) was conducted to obtain infrared spectra. The FTIR with 20 scans per second in the IR region (400 cm^{-1}- 4000 cm^{-1}) was used to investigate the absorption band of ferrites compounds particularly addressing to tetrahedral and octahedral absorption. The crystalline structure and size of ferrites was studied by XRD (Philips XL 40), with anode CuKa 1 radiation, 30 mA current, 40 kV voltage, and wavelength of 1.54060 nm scanning for 2θ= 10˚- 80˚, The incorporated EDAX analysis and SEM mapping was applied to obtain the atomic distribution on the surface of ferrites, while the TEM (JEM- 2100) with 200 kV high-resolution, was used to observe the morphology such as size, shape and arrangement of the lattice planes in the unit cell.

2.2 Fabrication of ferrites (Mg and Mn)

20.20 g of $Fe(NO_3)_3\cdot 9H_2O$, 6.41 g of $Mg(NO_3)_2\cdot 6H_2O$, and 9.61 g of $C_6H_8O_7$ were dissolved in deionised water and made up to 100 mL. The concentration of $Fe(NO_3)_3\cdot 9H_2O$:$Mg(NO_3)_2\cdot 6H_2O$:$C_6H_8O_7$ were in the ratio of 0.5 M: 0.25 M: 0.5 M. The solution mixture was stirred and heated at 60˚C for 3 h and followed by 80˚C, until the mixture changed to gel form. The gel was then dried in an oven at 100˚C for 24 h and followed by calcined in a muffle furnace at 300, 600, and 800˚C for 2h, respectively. Figure 2 shows the outline of the fabrication process. The similar treatment was done by replaced the $Mg(NO_3)_2\cdot 6H_2O$ with 2.17 g of MnO_2, with the concentration of $Fe(NO_3)_3\cdot 9H_2O$:MnO_2:$C_6H_8O_7$ in the ratio of 0.5 M: 0.25 M: 0.5 M [5]. Characterization was done by using XRD, FTIR, SEM-EDAX and TEM. The flow diagram of the fabrication process of Mg- and Mn- ferrites is presented in Figure 2.

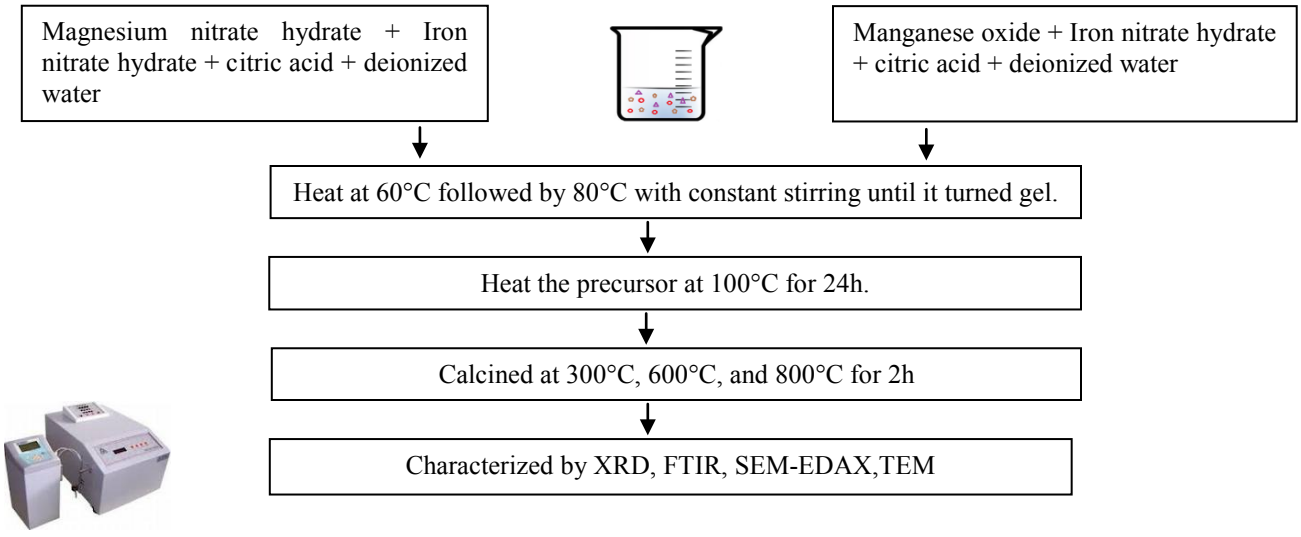

Fig. 2 The fabrication process of Mg- and Mn- ferrites.

3. RESULTS & DISCUSSION

3.1 XRD analysis

Figure 3.1 (a) and Figure 3.1 (b) show the diffractograms for both $MgFe_2O_4$ and $MnFeO_3$ at different temperatures (100, 300, 600 and 800°C) where both ferrites (Mg and Mn) still existed as amorphous materials at 100°C. As the temperature increased to 300°C the material structure of both ferrites (Mg and Mn) changed to semi-crystal with the appearance of some broaden peaks at certain 2θ (Bragg's angle), and when the calcinations continued to 600°C and 800°C both ferrites (Mg and Mn) existed in crystalline form with the existence of sharp peaks in characteristic patterns of Mg-ferrite and Mn-ferrite, respectively. On more detail examination, the formation of crystalline structure at 600°C was obtained to be faster for Mn-ferrites compared to Mg-ferrite assumed by more flexible Mn-ferrite related to several oxidation numbers belong to Mn element. T he higher thermal effect gave larger movement to atoms to do self rearrangement forming their crystalline structure.

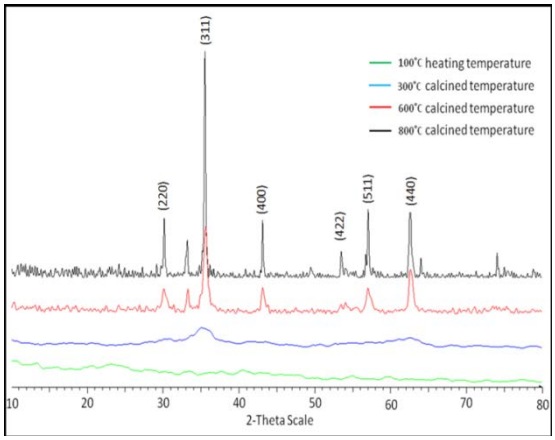

Fig. 3.1 (a) XRD patterns for $MgFe_2O_4$ at different temperatures (100, 300, 600, and 800°C). Sol gel method using citric acid surfactant.

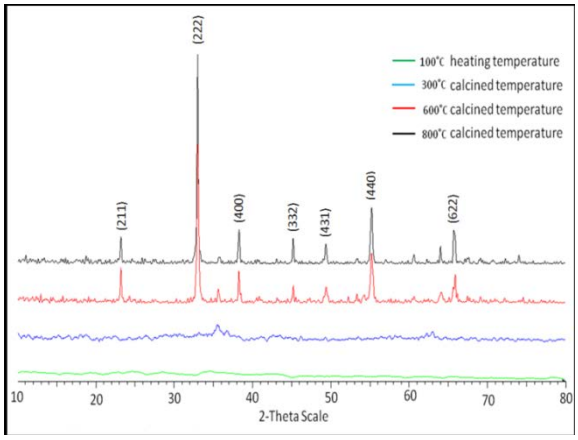

Fig. 3.1 (b) XRD patterns for $MnFeO_3$ at different temperatures (100, 300, 600, and 800°C). Sol gel method using citric acid surfactant.

3.2 FTIR analysis

Figure 3.2 (a) and Figure 3.2 (b) show the FTIR spectra for $MgFe_2O_4$ and $MnFeO_3$ which are observed in the range of 4000-400 cm^{-1}. Both figures show that many peaks which are responsible for different functional groups, appear in the 3600-1200 cm^{-1} range. For FTIR spectra of $MgFe_2O_4$, peak at 3421.77 cm^{-1} indicates the presence of O-H group, 2345.32 cm^{-1} corresponds to trace of adsorbed CO_2, 1384.64 cm^{-1} corresponds to NO_3^- and C-H bending appears in 850-1200 cm^{-1} [16,17]. When $MgFe_2O_4$ is calcined at 300°C, some functional groups in 4000- 1200 cm^{-1} are eliminated, whereas O-H and NO_3^- groups are retained in the structure due to stronger chemical bonding. When $MgFe_2O_4$ is calcined at 600°C and 800°C, all functional groups in 4000- 1200 cm^{-1} are eliminated. For $MnFeO_3$, at 100°C, the peak at 3393.33 cm^{-1} corresponds to O-H group, 1624.21 cm^{-1} corresponds to CO group, and 1384.49 cm^{-1} corresponds to NO_3^- group [5]. When $MnFeO_3$ is calcined at above 300°C, all functional groups in the range 3600- 1200 cm^{-1} are eliminated. This implies that manganese ferrite has more flexible structure, as manganese is a transition metal and has many oxidation states, whereas magnesium is an alkaline earth metal which only has +2 oxidation state, thus magnesium ferrite has more rigid structure. The existence of undesired functional groups will affect the conducting performance of the ferrites.

3.3 SEM – EDAX analysis

The elemental distribution on the surface of ferrites on exposed areas can be examined through EDAX analysis in couple interface with SEM. The distribution of an element in a compound is important as it will affect the conducting performance of ferrites in their applications. Table 3.1 shows the elemental distribution of Mg and Fe in $MgFe_2O_4$ surface where at higher temperature (300°C) the interested element concentrations is found higher than that at lower temperature (100°C), while the similar trend is also found for Mn and Fe distribution in the surface of $MnFeO_3$. However, as the thermal treatment was increased to 600°C, the element concentrations of both ferrites (Mg and Mn) have a t endency to reduce again except for Fe atomic concentration in $MgFe_2O_4$. The impressive phenomenon is encountered with the effect of thermal agitation yielded drifts in atomic movements causing instability in element

distribution on the material surface. However, with the special attention to the Fe distribution on the Mg-ferrite surface, it can be deduced from the more rigid structure of Mg-ferrite limited the Fe atomic movement in Mg-ferrite.

Having seen in SEM mapping demonstrated by Figure 3.3 (a) and Figure 3.3 (b) the distribution of Fe atoms on the surface of Mg-ferrites is likely to be denser and more homogeneous under the calcined temperature of 600°C compared to the one of 100°C. This phenomenon is confirmed by the results shown in Table 3.1 obtained from EDAX analysis where the concentration of Fe atoms is about 50% (600°C), which is almost as twice as the concentration of Fe atoms in lower temperature, i.e. approx. 26% (100°C). The mechanism can be elucidated from the thermal agitation where under the 100°C heating less Fe atoms get the chance to move toward the Mg-ferrite surface. Additionally, the rather rigid structure of Mg-ferrite prevents the mobility of atomic movement under lower temperature.

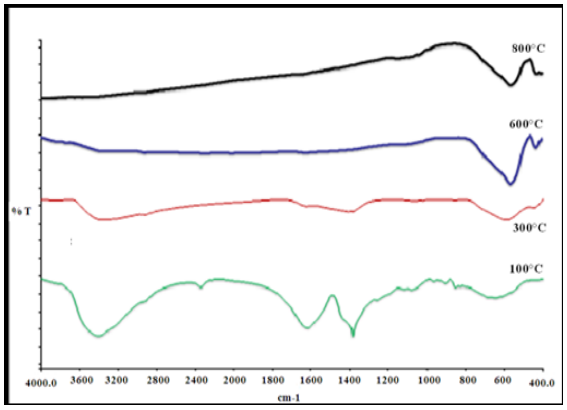

Fig. 3.2 (a) FTIR spectra for $MgFe_2O_4$ heated at 100°C, calcined at 300C, 600°C and 800°C

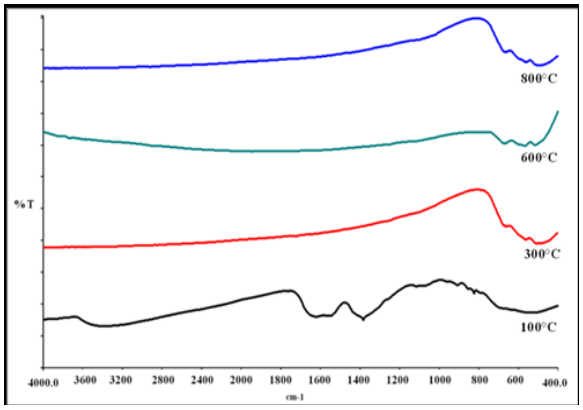

Fig. 3.2 (b) FTIR spectra for $MnFeO_3$ heated at 100°C, calcined at 300C, 600°C and 800°C

Table 3.1 The weight (%) of metal distribution on the surface of ferrites (Mg and Mn) at interested temperatures (100, 300 , 600 and 800°C).

Temperature (°C)	Mg/ $MgFe_2O_4$ (%)	Fe/ $MgFe_2O_4$ (%)	Mn/ $MnFeO_3$ (%)	Fe/ $MnFeO_3$ (%)
100	5.11	26.17	22.89	22.21
300	8.56	50.70	30.33	30.25
600	6.11	50.62	18.97	18.46
800	7.43	59.57	27.92	26.83

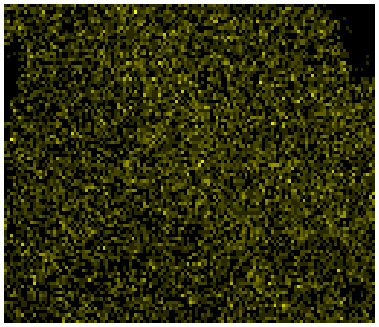

Fig. 3.3 (a) SEM mapping of Mg-ferrite for Fe distribution at 100°C.

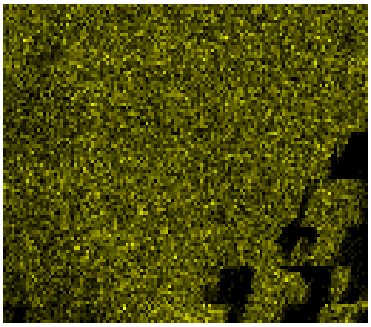

Fig. 3.3 (b) SEM mapping of Mg-ferrite for Fe distribution at 600°C.

On the other hand, a different trend is found for the distribution of Mn atoms under different thermal treatment, i.e. at 100°C and 600°C, as shown by Figure 3.3 (c) and Figure 3.3 (d). The distribution of Mn atoms at the surface of Mn-ferrite is likely to be unaffected by increasing temperature from 100°C to 600°C. Regarding the values in Table 3.1 obtained from EDAX analysis, it seems that the concentrations of Mn atoms on the surface of Mn-ferrites are not too varied by altering the temperatures from 100°C to 800°C. Therefore, the concentration of Mn atoms at the Mn- ferrite surface are found to be around 23% (100°C) and 19% (600°C). The effect of temperatures does not change remarkably the concentration value of Mn atoms as confirmed by the results shown in Table 3.1. This phenomenon probably can be elucidated by the flexibility of Mn-ferrite structure with several oxidation numbers possessed by manganese element in the periodic table and their perovskite nature [18]. As a result, it is possible that at higher temperature (600°C) the concentration of Mn atoms is a little higher than that one at lower temperature (100°C) as demonstrated by the SEM mappings in Figure 3.3 (c) and Figure 3.3 (d).

Having compared the concentration of Fe atoms in the surface of Mg-ferrite and Mn-ferrite, respectively, as shown from the SEM mappings exhibited in Figure 3.3 (e) and Figure 3.3 (f), the scattering of Fe atoms in Mn-ferrite surface looks more uniform compare to that one posed by the scattering of Fe atoms in Mg-ferrite. However, from the data listed in Table 3.1 obtained by EDAX analysis, the concentration of Fe atoms in Mg-ferrite at 800°C (i.e. ≈ 59%) is found as more than twice higher as the concentration of Fe atoms in Mn-ferrite at 800°C (i.e. ≈ 27%), it indicates a higher density found for Fe atoms on the surface of Mg-ferrite encountered with the more rigid structure of Mg-ferrite due to Mg alkaline earth element hindered the mobility of Fe atomic movements.

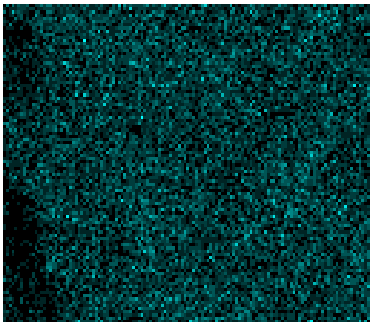

Figure 3.3 (c): SEM mapping of Mn-ferrite for Mn distribution at 100˚C.

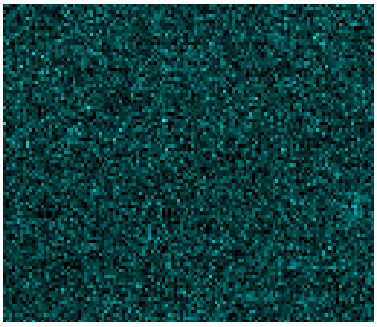

Figure 3.3 (d): SEM mapping of Mn-ferrite for Mn distribution at 600˚C.

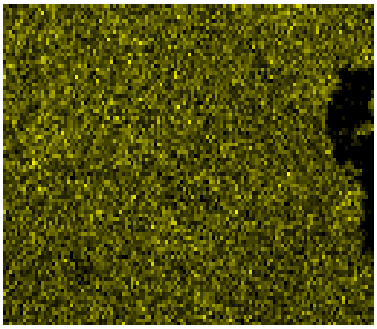

Figure 3.3 (e): SEM mapping of Mg-ferrite for Fe distribution at 800˚C

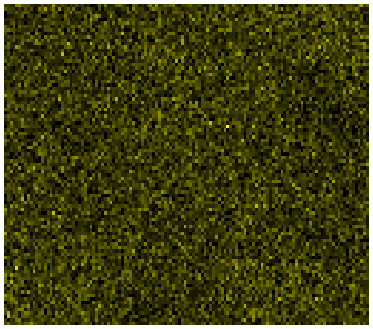

Figure 3.3 (f): SEM mapping of Mn-ferrite for Fe distribution at 800˚C

3.4 TEM Analysis

The results from XRD, FTIR and SEM-EDAX analyses show that ferrites are successfully formed under 600˚C calcinations. Figure 3.4 (a) and Figure 3.4 (b) show the TEM images using Fast Fourier Transformation method for $MgFe_2O_4$ and $MnFeO_3$ calcined under 600°C, respectively. Mo reover, the TEM image of Mg-ferrite shows a concentrated atomic mass in the exposed region in the bulk structure, while the TEM image of Mn-ferrite demonstrates a scattering atomic concentration in the exposed part in the Mn-ferrite bulk structure. T he TEM images verified that in the bulk region under 600°C calcination, the distribution of atomic concentration in Mn-ferrite is more uniform in the bulk part, while the atomic distribution in the bulk region of Mg-ferrites is much less uniform and rather concentrated at the exposed region. This phenomenon is unsurprising since the mobility of atomic

movement is much greater found in Mn-ferrites rather than the corresponding Mg-ferrite, which is going back to the chemical properties of Mn transition element with several oxidation numbers and Mg alkaline earth element.

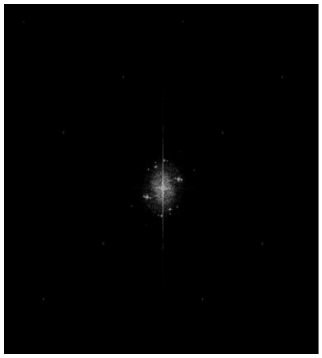

Fig. 3.4 (a) TEM micrograph of Mg-ferrite at 600˚C.

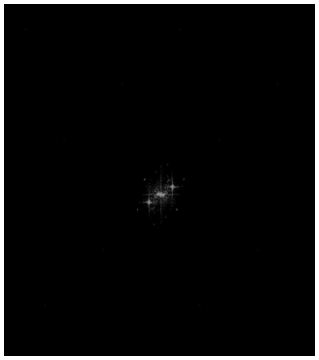

Fig. 3.4 (b) TEM micrograph of Mn-ferrite at 600˚C.

4 CONCLUSION

The sol gel method applying citric acid anionic surfactant has successfully fabricated the Mg- and Mn-ferrites at 600˚C and 800°C calcinations. F rom the characteristic study, it has showed that the atomic movement found much greater for Mn-ferrites during the thermal treatment encountered with the more flexibility structure of Mn-ferrites correlated with Mn oxidation numbers compared to the more rigid structure of Mg-ferrites. Therefore, the sol gel method gives more advantage on the synthesis of Mn-ferrites on this respective case.

ACKNOWLEDGEMENT

The authors thank the Faculty of Science, Ibnu Sina Institute, Faculty of Mechanical Engineering of Universiti Teknologi Malaysia, Johor for applying the XRD, FTIR, SEM-EDAX, and TEM facilities to FAV Grant (vote no:77545) and GUP tier 2 (vote no:02J02) under RMC-UTM for funding the project.

REFERENCES

[1] M. Siemons, Th. Weirich, J. Mayer, and U. Simon, Preparation of Nanosized Perovskite- Type Oxide via Polyol Method, 630 (2004), 2083-2089.

[2] T. Wolfram and S. Elliatioglu, Electronic and Optical Properties of d- Band Perovskte, United Kingdom, University Press, Cambridge, 2006, 1-24.

[3] R.J. Willey, P. Noirclerc and G. Busca, Chem. Eng. Commun. 123 (1993), Doi:10.1080/00986449308936161

[4] S. Maensiri, M. Sangmanee, and A. Wiengmoon, Magnesium Ferrite ($MgFe_2O_4$) Nanostructure Fabricated by Electrospinning, 4 (2008), 221-228.

[5] M. G. Naseri, E.B. Saion, H.A. Ahangar, M. Hashim, and A. H. Shaari, Synthesis and Characterization of Manganese Ferrite Nanoparticles by Thermal Treatment Method, 323 (2011), 1745-1749.

[6] K. Hirota, K. Saruwatari, M. Kato, K. Nakade, and M. Yoshinaga, Low-Temperature Sintering of $Mg(Fe_{1-x}Mn_x)O_4$ ($0 \leq x \leq 0.4$) Ferrites Powders Prepared via Citric Acid Route, 49 (2008).

[7] S. Darshane and I.S. Mulla, The Influence of Palladium on Gas Sensing Performance of Magnesium Ferrite Nanoparticles, 119 (2009), 319-323

[8] A. Pradeep and G. Chandrasekaran, FTIR study of Ni, Cu and Zn Substituted Nano- particles of $MgFe_2O_4$, 60 (2005), 371-374.

[9] C. P. Liu, M. W. Li, C. Zhong, J. R. Huang, Y. L. Tian, L. Tong, and W. B. Mi, Comparative Study of Magnesium Ferrite Nanocrystallites Prepared by Sol–Gel and Coprecipitation Methods, 42 (2007), 6138-6138.

[10] M. H. Mahmoud, H. H. Hamdeh, J. C. Ho, M. J. O'Shea, and J. C. Walker, Mossbauer Studies of Manganese Ferrite Fine Particles Processed by Ball Milling, 220 (2000), 139-146.

[11] S. K. Pradhan, S. Bidb, M. Gateshki, and V. Petkov, Microstructure characterization and Cation Distribution of Nanocrystalline Magnesium Ferrite Prepared by Ball Milling, 93 (2005), 224-230.

[12] Z. Z. Lazarevic, C. Jovalekic, A. Recnik, V. N. Ivanovski. M. Mitric, M. J. Romcevic, N. Paunovic, B. D. Cekic,and M. J. Romcevic, Study of Manganese Ferrite Powders Prepared by Soft Mechanochemical Route, 509 (2011), 9977-9985.

[13] R. D. K. Misra, S. Gubbala, A. Kale, and W. F. Egelhoff Jr, A Comparison of the Magnetic Characteristics of Nanocrystalline Nickel, Zinc, and Manganese Ferrites Synthesized by Reverse Micelle Technique, 111 (2004), 164-174

[14] S. Mishra, T. K. Kundu, K. C. Barick, D. Bahadur, and D. Chakravorty, Prepare Nanocrystalline $MnFe_2O_4$ by Doping with Ti^{4+} Ions Using Solid-State Reaction Route, 307 (2006), 222-226.

[15] M. M. Rashad, Synthesis and Magnetic Properties of Manganese Ferrite from Low Grade Manganese Ore, 127 (2006), 123-129.

[16] A. Pradeep, P. Priyadharsini, and G. Chandrasekaran, Sol-gel route of synthesis of nanoparticles of $MgFe_2O_4$ and XRD, FTIR and VSM study, 320 (2008), 2774-2779.

[17] V. P. Tolstoy, I. V. Chernyshova, and V. A. Skryshecsky, Handbook of Infrared Spectroscopy of Ultrathin Films, John Wiley & Sons, Inc., United States of America, Hoboken, New Jersey, 2003, 670-686.

[18] N. Alexandra and J. W. Donald, Perovskite: A structure of Great Interest to Geophysical and Materials Science. United States of America, American Geophysical Union, Washington, D.C, 2000, 91-98